

Zaiemyek, Zahra, Liaghat, Gholamhossein and Khan, Muhammad K (2021) Effect of Al₂O₃ nanoparticles on the mechanical behaviour of aluminium-based metal matrix composite synthesized via powder metallurgy. *Proceedings of the Institution of Mechanical Engineers, Part L: Journal of Materials: Design and Applications*, 235(10), pp. 2340-2355. Copyright © 2021 IMechE. DOI: 10.1177/14644207211033626

Effect of Al₂O₃ Nanoparticles on the Mechanical Behaviour of Aluminium Based Metal Matrix Composite Synthesized via Powder Metallurgy

Zahra Zaiemyekeh¹, Gholamhossein Liaghat^{1,2}, Muhammad. K. Khan³

¹ Department of mechanical engineering, Tarbiat Modares University, Tehran, P.O. Box: 14115-111, Iran

² Schools of Mechanical & Aerospace Engineering, Kingston University, Surrey KT1 1LQ, London, UK

³Institute of Future Transport and Cities, Coventry University, Coventry, CV1 5FB, UK

Zahra Zaiemyekeh (zahrazaiem@modares.ac.ir)

Gholamhossein Liaghat: ghlia530@modares.ac.ir, Gholamhossein.Liaghat@kingston.ac.uk

Abstract

The effects of variation in aluminium oxide nanoparticles in aluminium-based metal matrix composite on the compressive and sliding wear deformation have been investigated. The compressive and sliding wear resistance of the composite increase significantly with the addition of nanoparticles in the matrix. The 5% aluminium oxide nanoparticles in the composite were found to be the optimal weight fraction of added nanoparticles that produced higher static yield strength, hardness, scratch resistance and lower material loss in wear in the composite. The addition of nanoparticles, beyond 5% weight fraction, in the matrix showed adverse effects in the performance of the composite due to its higher brittleness. The effects on wear properties of the composite with added nanoparticles beyond optimal weight fraction were more detrimental than those with lower weight fraction of nanoparticles.

Keywords: metal matrix composites (MMCs); alumina powder; powder metallurgy; tribological behaviour; material properties

1. Introduction

Aluminium alloys are widely used in engineering applications owing to their low density and higher elongation at failure which make them an ideal material for light weight components in the aerospace, automobile, and locomotive industries. One disadvantage of aluminium and its alloys is their lower elastic-plastic properties which result in lower resistance against fretting, wear, and impact loading ^{1, 2}. The addition of hard nanoparticles in pure aluminium and its alloys to form metal matrix composites (MMCs) is an attractive solution to increase their elastic-plastic properties for use in high strength parts of excellent physical, chemical and mechanical properties of the materials are expected ³⁻⁵. The use of metal matrix composites in light weight transport sector can provide significant benefits in the improvement of the life of the components, lower energy and maintenance requirements, and lower emissions levels. These composites are preferred in high temperature applications that involve high temperatures such as thermal barrier coatings, turbine engines, and piston rod, ⁶⁻⁸. Whilst it is possible to develop MMCs of various metals and alloys; aluminium and its alloys are more suitable matrix material for the addition of nanoparticles to develop MMCs owing to their low density, high strength to weight ratio and lower cost which are the main selection criteria in light-weighting ⁹⁻¹¹. The silicon carbide, aluminium oxide (alumina), and boron carbide nanoparticles are commonly used with aluminium alloys based matrix due to their homogenous bonding with aluminium and its alloys which help in uniform load transfer in structural applications ^{6, 12}. The most important challenge for the qualification of MMCs to use in engineering applications is their consistent material properties. The uniform and homogenous distributions of nanoparticles in a bulk matrix are extremely important to achieve reliable and consistent mechanical behaviour of the material. Powder Metallurgy (PM) is a useful method to produce MMCs with uniformly distributed nanoparticles in the matrix which helps in overcoming the widely known problems with MMCs such as wetting and lower interface bonding between reinforcement and matrix material as other fabrication techniques use liquid molten metals ¹³. The PM based fabrication process of MMCs initially mixes the metal and nanoparticle powders followed by cold or hot compaction and sintering ^{14, 15}. The process parameters are selected based on the reinforcement particle size, their weight fraction and distribution in the matrix. The smaller size nanoparticles are preferred in engineering applications due to their wide reach in the matrix and interfacial bonding with a matrix which helps in achieving uniform and homogenous static and wear properties of the MMCs ¹⁶⁻¹⁸. However, finding the right weight fractions of nanoparticles in the matrix, with equally good material properties in static and wear

applications of composite, is not straightforward. The variation in the weight fraction of nanoparticles is directly linked with the mechanical behaviour of MMCs and their deformation mechanism.

The mechanistic understanding of the deformation of nanoparticles and different matrix systems is still empirical and case by case experimental investigations are carried out to discern the optimal weight fraction of nanoparticles in a MMC with consistent mechanical performance in static, dynamic, fretting, and impact loads ¹⁹⁻²². Mohammed *et al.* ²³ investigated the mechanical performance of aluminium matrix reinforced with 5, 10 and 15% Al₂O₃ particles. The specimens with 5% Al₂O₃ found to have the highest hardness and compression strength. Rahimian *et al.* ²⁴ showed a higher wear resistance of Al₂O₃ nanoparticles in the aluminium matrix when used a higher weight fraction of large size nanoparticles. Eltaher *et al.* ²⁵ investigated the mechanical and wear properties of aluminium-magnesium dual-matrix reinforced with Al₂O₃ particles. They concluded that the addition of Al₂O₃ in the dual matrix composite increased the compressive strength and hardness of the material and decreased the wear rate 2.7 times. Al-Jaafari ²⁶ investigated the mechanical performance of aluminium matrix reinforced with different particle sizes of Al₂O₃. It was concluded that small size particles of Al₂O₃ were more efficient in improving the ultimate tensile strength (UTS) and hardness of the composite. Aydin ²⁷ investigated the wear rate of 7075 aluminium reinforced with Al₂O₃ nanoparticles of 0.3 μm, 2 μm, and 15 μm size. The 5% weight fraction of 5 μm Al₂O₃ nanoparticles showed the lowest wear of the composite. It was also concluded that an increase in the applied load and sliding speed increased the wear severity by changing the wear mechanism from abrasion to delamination. Bharath *et al.* ²⁸ investigated the wear performance of 2014 aluminium reinforced with 9% weight fraction of 20 μm Al₂O₃ nanoparticles. The wear rate of composite found to be higher at higher contact loads. Qutub *et al.* ²⁹ and Rahimian *et al.* ³⁰ showed a higher wear resistance of the Al₂O₃ nanoparticles in aluminium matrix using a higher weight fraction of large size nanoparticles. They showed a variable wear resistance of the composite and found a lower wear resistance of the material when tests were conducted at higher contact loads and lower sliding distance. Lakshmikanthan *et al.* ³¹ found that the mechanical and tribological performance of the A357 alloy can be improved with the addition of dual size SiC particles in the material. They showed that different weight fractions of large and small size nanoparticles lead to different effects on the tensile strength, hardness and wear rate of the alloy and there was no unique weight fraction which increased all mechanical properties.

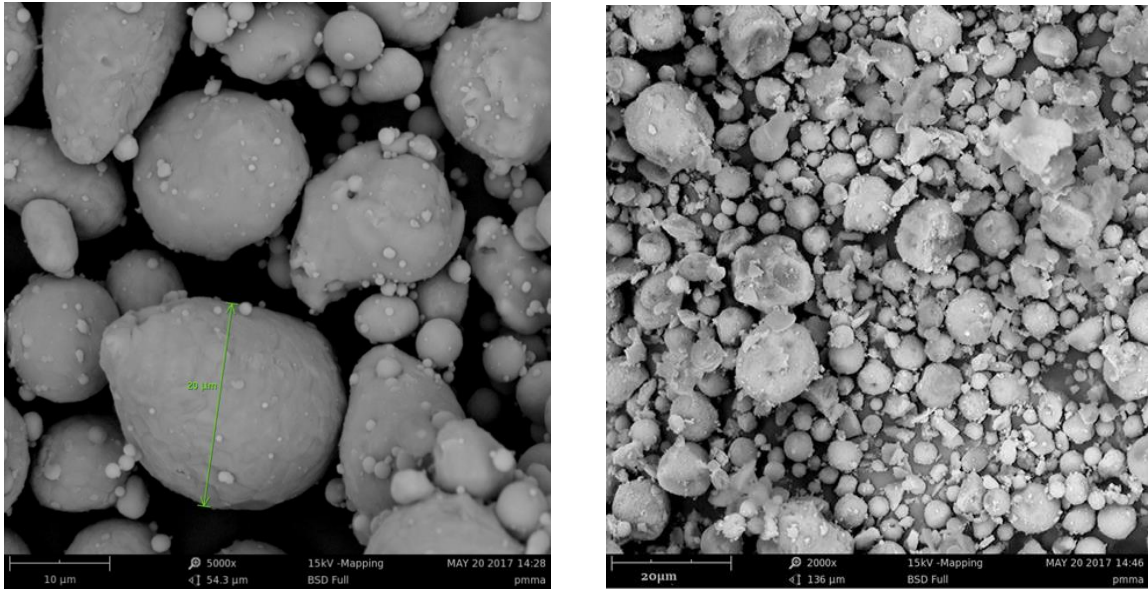
In these studies, It has been found that blending of a specific weight fraction of nanoparticles in aluminium or other element based matrix can increase the yield strength, hardness, wear resistance, and energy absorption as compared to the matrix ^{19, 20, 32, 33}. The addition of insufficient nanoparticles in the matrix does not adequately influence the material properties. Likewise, the excessive weight fraction of the nanoparticles develops brittleness and agglomeration in the material. The optimal weight fraction of the nanoparticles that produce the desired material properties of composite varies with the type of matrix, size of nanoparticles, and elastic-plastic properties of matrix and nanoparticles. The effects of increased hardness on the wear resistance and variation of the wear resistance of the MMC at different contact loads and sliding speeds are also not understood thoroughly.

In this study, we present the mechanistic understanding of the deformation behaviour of Al₂O₃ reinforced aluminium composites in quasi-static compression and sliding wear. The composite specimens were fabricated with powder metallurgy by adding different weight fractions of nanoparticles in the pure aluminium matrix. The material with an optimum weight fraction of the aluminium oxide nanoparticles in the aluminium matrix was found to show higher static yield strength, hardness, scratch resistance, and lower material loss in wear. It was concluded that careful investigation of the fracture and deformation behaviour of material led weight fraction selection of nanoparticles in the matrix can produce the MMC of higher compressive strength, hardness, and wear resistance. The results obtained are very useful in developing the mechanistic understanding of the role of aluminium oxide nanoparticles in the deformation mechanism of aluminium matrix in static and wear load. This will serve as a precursor for the development of a mathematical model for the prediction of the static and wear properties of nanoparticles reinforced MMCs with various matrix types, the weight fraction of nanoparticles, and contact loads.

2. Materials and experimental procedure

2.1. Materials

A 97.8% pure aluminium powder having a particle size 20 μ m was used as a matrix material for mixing 20nm Al₂O₃ nanoparticles as reinforcement particles. Fig. 1 shows the morphology of aluminium and Al₂O₃ powders. The chemical composition of aluminium and Al₂O₃ powder is shown in Table. 1.



(a)

(b)

Fig. 1. SEM micrographs of Al and Al₂O₃ powders (a) Al and (b) Al₂O₃

Table 1. Chemical composition of Al and Al₂O₃ powder

Materials	Element Content (%)
Al	Al: 97.8, Na: 1.4, Cu: 08
Al ₂ O ₃	O: 66.8, Al: 28.4, N: 3.7, Na: 1.2

2.2. Fabrication process

The MMC was developed by adding 2.5 to 10 % weight fraction of Al₂O₃ alumina powder in the aluminium using a powder metallurgy process. The aluminium matrix and Al₂O₃ nanoparticles were initially mixed for 30 min at a speed of ~2000 rpm. The mixture was then cold pressed in a cylindrical die at ~ 600 MPa uniaxial pressures, as shown in Fig. 2 (a), to form green compacts. Zinc stearate was used as a lubricant to reduce the friction between the die wall and the punch. The manufactured green compacts have a diameter (15 mm) to length ratio of one. The sintering temperature of 620°C was used to remain consistent with previous studies on aluminium matrix reinforced with Al₂O₃^{1, 34-36}. In this study, the compact blocks of the material sintered in argon at 620°C for 90 mins at a heating rate of 20°C/min, as shown in Fig. 2 (b). The samples were then cooled in the room environment.



(a)



(b)

Fig. 2. Equipment used in powder metallurgy process (a) cold press device (b) furnace

2.3. Mechanical tests

2.3.1. Uniaxial compression test

The quasi-static uniaxial compression tests were conducted at a strain rate of $10^{-3} s^{-1}$ corresponding to 9mm/min crosshead speed of a universal testing machine according to the ASTM-E9 standard ³⁷. Cylindrical specimens of 15mm length and diameter were prepared. The surfaces of the specimens were carefully polished to avoid any misalignment in the compression tests. The lubricant was applied to the interfaces between the specimen and the loading plates to reduce the friction. Three specimens were used for compression testing to ensure reliable results.

2.3.2. Abrasive wear test

Dry sliding wear tests were conducted using a conventional pin-on-disc testing machine at room temperature following the ASTM G99-05 standard ³⁸. The pin-on-disc sliding wear test is used on materials to probe their tribological deformation behaviour and friction characteristics. The mechanistic understanding of tribological and friction properties of the low-density materials, like aluminium and its alloys, are essential before their use in high performance engineering components. A schematic representation of the pin-on-disc test

apparatus is shown in Fig. 3. In this test, a spherical pin is brought in contact with the sample with a contact load. The sample is rotated at a selected speed which forms a friction track on the sample.

A steel pin of 15 mm diameter and 15 mm height was used in the tests. The samples' surface and the pin were polished before the sliding wear test to attain a uniform surface roughness. The wear tests were carried out at normal contact loads 10, 15 and 20 N. The wear tests were carried out at two sliding speeds of 1.5 and 2 m/s^{-1} . The sliding distance of 200 m was used in the tests. A new pin was used in each test. Weight loss in the wear test was measured by an electronic weighing balance with a sensitivity of 0.1 mg by the weight difference of the samples before and after the tests. The tests were carried out on three samples at every condition to ensure the reliability of the results and average values were used for the analysis. During the wear tests, the normal contact force F_N was used in the wear test and the coefficient of friction (COF) between the pin and sample surface was determined from the applied contact load. The worn surfaces of the samples were examined in a Scanning Electron Microscope (SEM) for the determination of the wear mechanism of the composite.

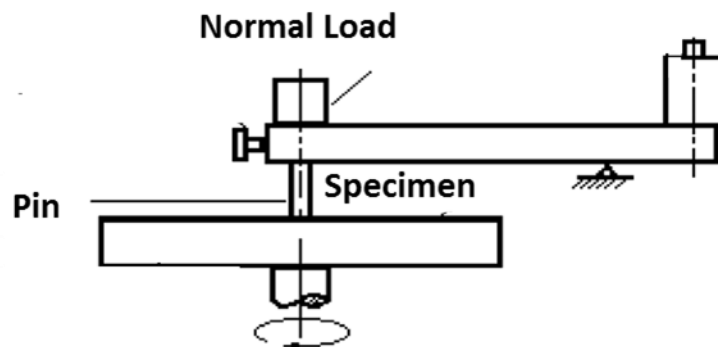


Fig. 3. A schematic illustration of the pin-on-disc wear test apparatus

2.3.3. Vickers hardness test

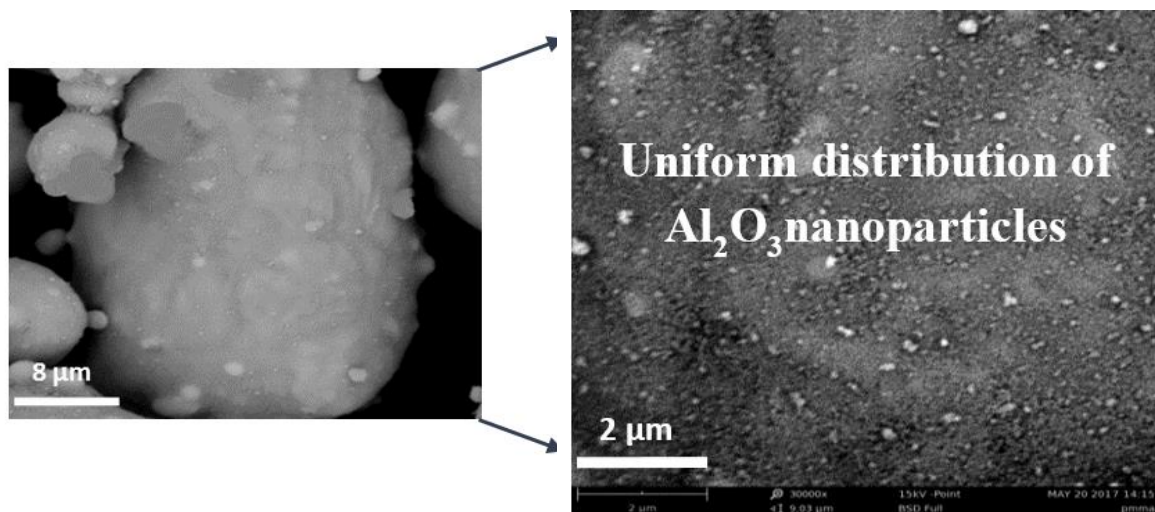
Vickers micro-hardness testing was carried out on samples following ASTM E384 standard³⁸. An applied load of 100g was applied to the samples for 15s in the hardness test. The tests were repeated five times to ensure the reliability of the results.

3. Results and discussion

3.1. Microstructural and elemental study of the Composite

The uniform distribution of nanoparticles in the matrix is extremely important for the consistent physical and mechanical properties of the metal matrix composites. The distribution of the Al_2O_3 reinforcement particles in the aluminium matrix, before and after PM, was investigated by the Scanning Electron and Optical Microscope. The morphology of mixed aluminium and Al_2O_3 nanoparticles before the fabrication process is shown in Fig. 4. Fig. 4 (a) shows the micrograph of mixed powder in a sample with 5% Al_2O_3 and Fig. 4 (b) shows its high magnification image. It can be seen that Al_2O_3 powder was thoroughly mixed with the aluminium matrix. However, the nanoparticles showed agglomeration in samples with a higher weight fraction of Al_2O_3 particles. Fig. 4 (c) shows the micrographs of mixed powder in a sample with 10% Al_2O_3 and Fig. 4 (d) shows its high magnification image. The agglomeration was found lower in the sample with 7.5% Al_2O_3 which increased substantially in the sample with 10% Al_2O_3 .

The microstructure of the composite developed was investigated with optical microscopy. Metallographic samples were prepared from standard grinding and polishing procedure to obtain 1 μm surface finish. The polished samples were etched with a solution containing 25ml each of methanol, nitric acid, hydrochloric acid and one drop of hydrofluoric acid. Fig. 5 shows the microstructure of samples reinforced with 5 and 10% Al_2O_3 nanoparticles. The microstructure was found to have high-density porosities in the material. The specimens with the higher weight fraction of Al_2O_3 nanoparticles found to have higher porosity. The distribution of the Al_2O_3 nanoparticles was found to be uniform in the aluminium matrix. Energy Dispersive Spectrometry (EDS) analysis was used to determine the chemical composition of the composite. Fig. 6 shows the EDS spectra of the material where the composition of the material was found to have aluminium and oxygen as the main elements.



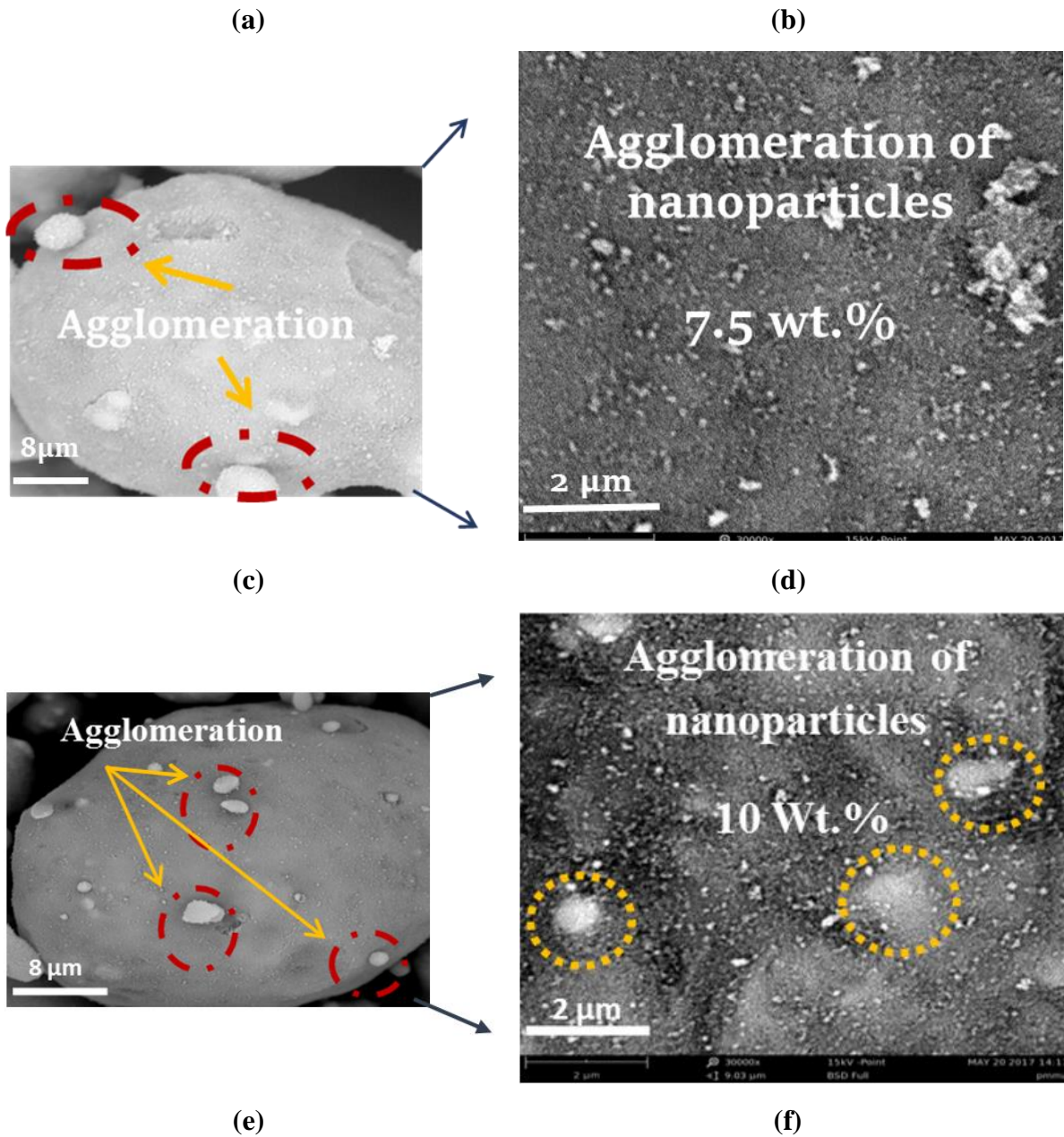


Fig. 4. SEM micrographs of the mixed powders (a) 5% Al₂O₃ in aluminium (b) High magnification SEM graph of 5% Al₂O₃ in aluminium (c) 7.5% Al₂O₃ in aluminium and (d) High magnification image of 7.5% Al₂O₃ in aluminium (e) 10% Al₂O₃ in aluminium and (f) High magnification image of 10% Al₂O₃ in aluminium

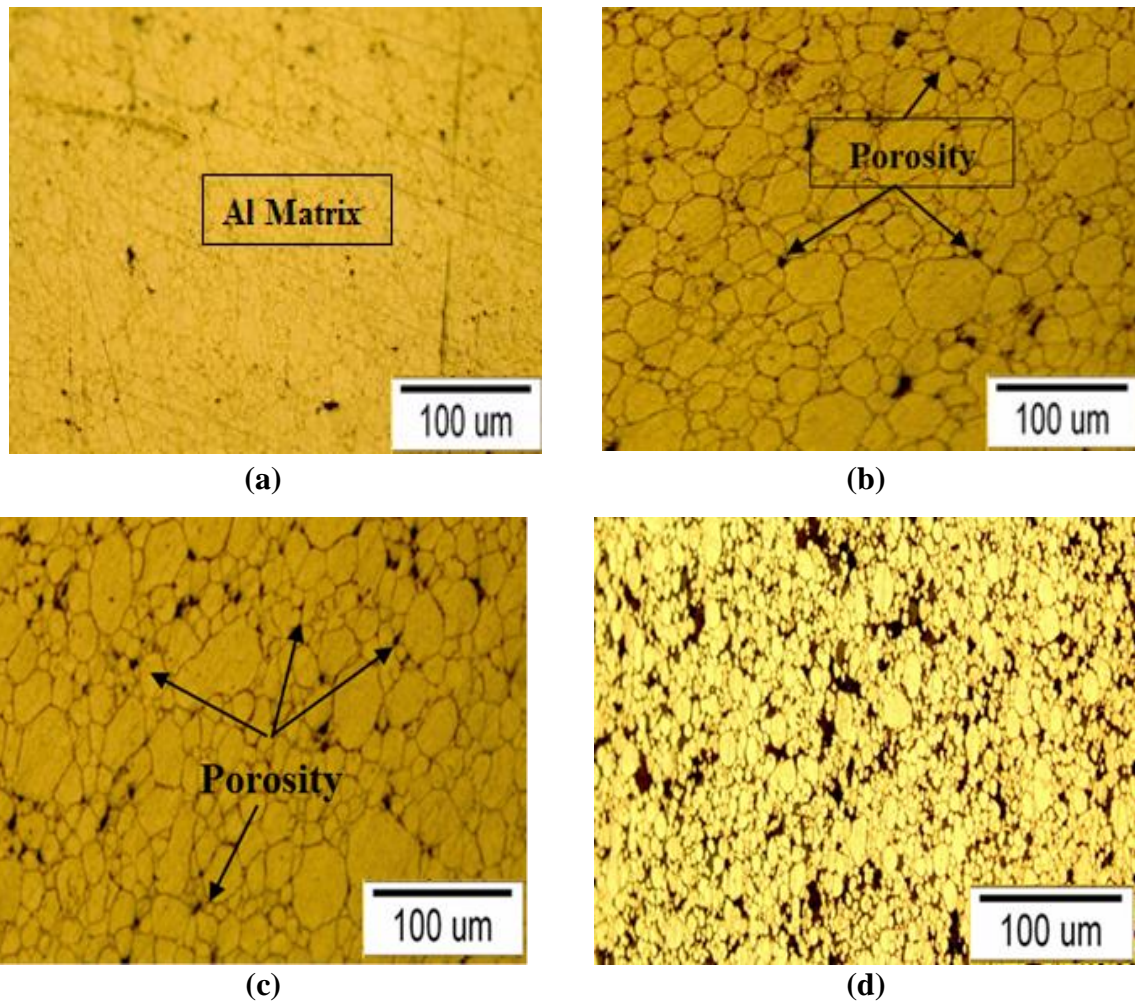


Fig. 5. The microstructure of the composites reinforced with (a) aluminium matrix without added nanoparticles (b) 2.5% Al₂O₃ (c) 5% Al₂O₃ and (d) 10% Al₂O₃

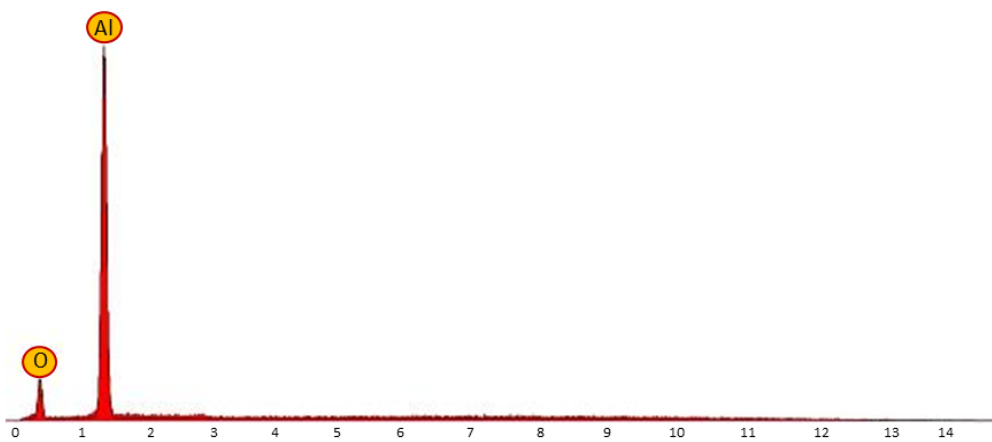


Fig. 6. Energy Dispersive spectrum of a composite sample with 10% Al₂O₃

3.2. Density of the Al-Al₂O₃ Metal Matrix Material

The variation in the powder morphology of matrix and nanoparticles affects the mechanical properties of the composites. The difference in the weight fraction of nanoparticles in the matrix alters the density of the material resulting in the variation of mechanical properties of the composites^{39,40}. The density of the prepared samples was measured experimentally using ASTM B328 standard⁴¹ and then compared with the theoretical density of the powder mixtures. The percentage relative density of the material was obtained by comparison of experimental and theoretical densities using the equation 1. Fig. 7 shows the variation in the relative density with Al₂O₃ weight fraction in the samples. It was found that the addition of nanoparticles in the matrix decreased the relative density of the composite. The samples with a higher weight fraction of Al₂O₃ nanoparticles found to have high-density porosities in the material, as shown in Fig. 5. The porosities in the material are not considered in the theoretical density of the material which led to a continuous decrease in the relative density of the material with an increase in the weight fraction of Al₂O₃ nanoparticles.

$$\text{Relative density (\%)} = \frac{\text{Experimental density}}{\text{Theoretical density}} \times 100. \quad (1)$$

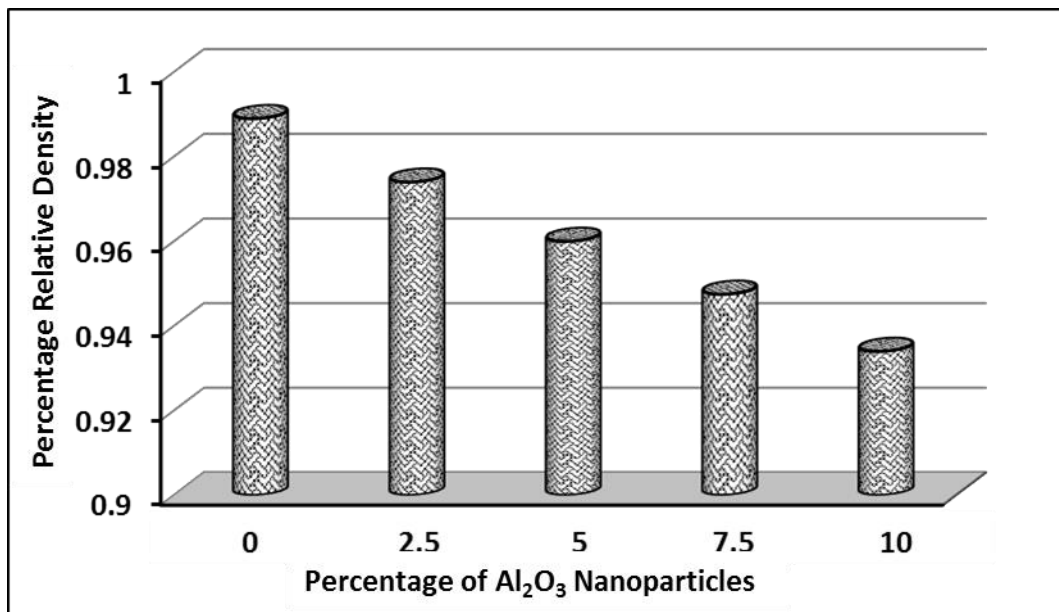


Fig. 7. Variation in the relative density of the composite with weight fraction of Al₂O₃ nanoparticles

3.3. Quasi-static compressive behaviour of composite

Fig. 8 shows the quasi-static compressive stress-strain curves of the composite with and without added Al₂O₃ nanoparticles in the aluminium matrix. The stress-strain curves of the composites were found to have three different stages of deformation. The compression in the

samples starts with a stiff and elastic deformation showing a linear increase in strain with stress up to the yield stress. The samples with added nanoparticles showed a steeper elastic part in the compression than a pure aluminium sample. The samples with added nanoparticles showed a higher elastic modulus and yield strength as compared to a pure aluminium sample ⁴². The plastic deformation of samples initially showed a stress plateau with the continuous increase in strain without an increase in the stress. In the last part of the deformation, a sharp increase in stress without an increase in the strain was observed. The plateau stress effect was not observed in samples containing any or lower weight fraction of Al₂O₃ nanoparticles. The deformation of powder metallurgy based metal matrix composites is divided into three stages named as a primary, secondary and tertiary stage ^{43, 44}. In the primary stage, a high growth rate of elastic deformation is obtained. In the secondary stage, the plasticity in the ductile aluminium matrix starts as damage initiation which grows in the deformation process to form voids. The progressive void formation is reflected in the form of a stress plateau in the plastic deformation. These void coalescences in the last part of the secondary stage to form large cracks. The third stage of the deformation shows a sample barrelling phenomenon in which hard Al₂O₃ nanoparticles fracture completely after absorbing a considerable amount of energy. In this stage, a sharp increase in the stress followed by plateau stress is observed which can be attributed to the densification of the samples in compression. Fig. 9 shows the variation in the compressive yield strength of the composites with the weight fraction of added nanoparticles. The addition of Al₂O₃ nanoparticles in the matrix increased the yield strength of composites. The highest yield strength of the composites was found for a 5% weight fraction of added nanoparticles when it reached to ~80MPa. However, the yield strength of the composite started to decrease with the further addition of nanoparticles beyond the 5% weight fraction. The samples with a 10% weight fraction of Al₂O₃ nanoparticles found to show a similar yield strength that was found for samples without Al₂O₃ nanoparticles. It can be said that the addition of nanoparticles up to a specific limit increase the compressive behaviour of composite. The excessive weight fraction of added nanoparticles increases the porosity in the samples leading to a lower compressive yield strength of the composite ²³, . The higher fraction of porosity in the samples acts as the potential sites for stress concentration and crack initiation leading to the lower strength of the composite ⁴⁵.

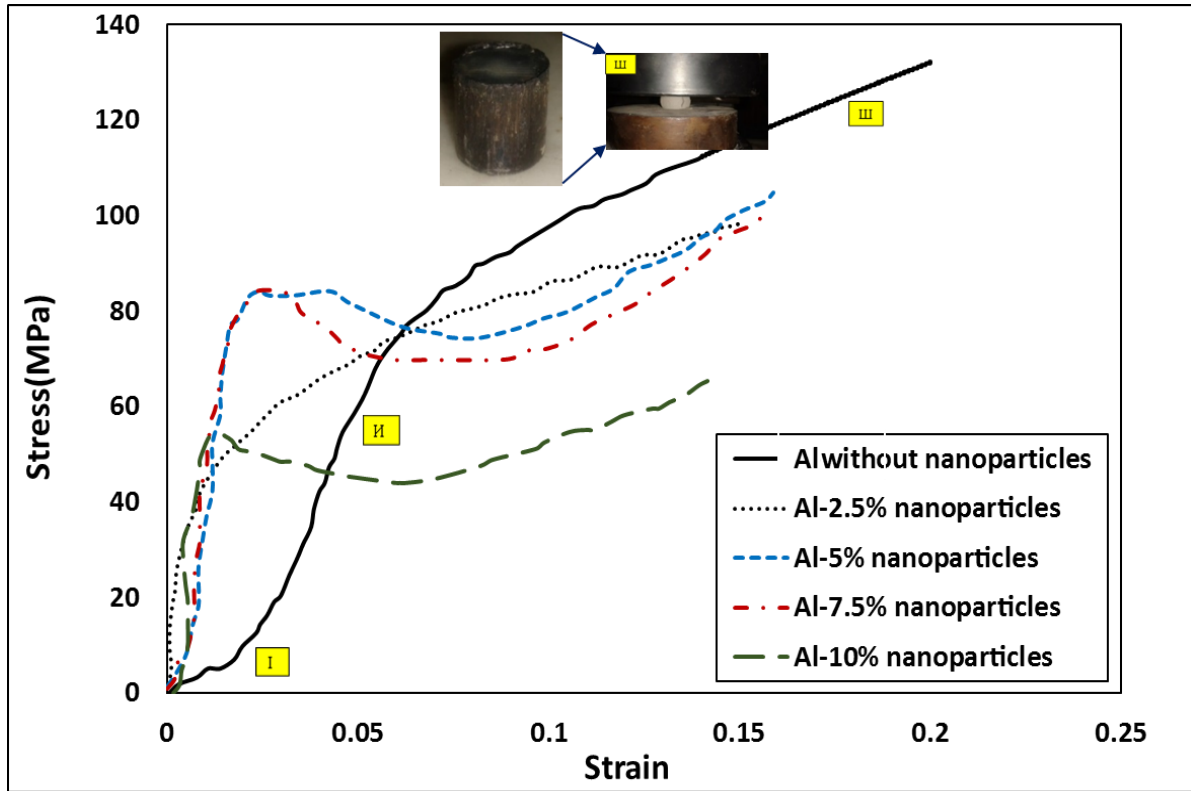


Fig. 8. Quasi-static stress-strain curves of pure aluminium and composites

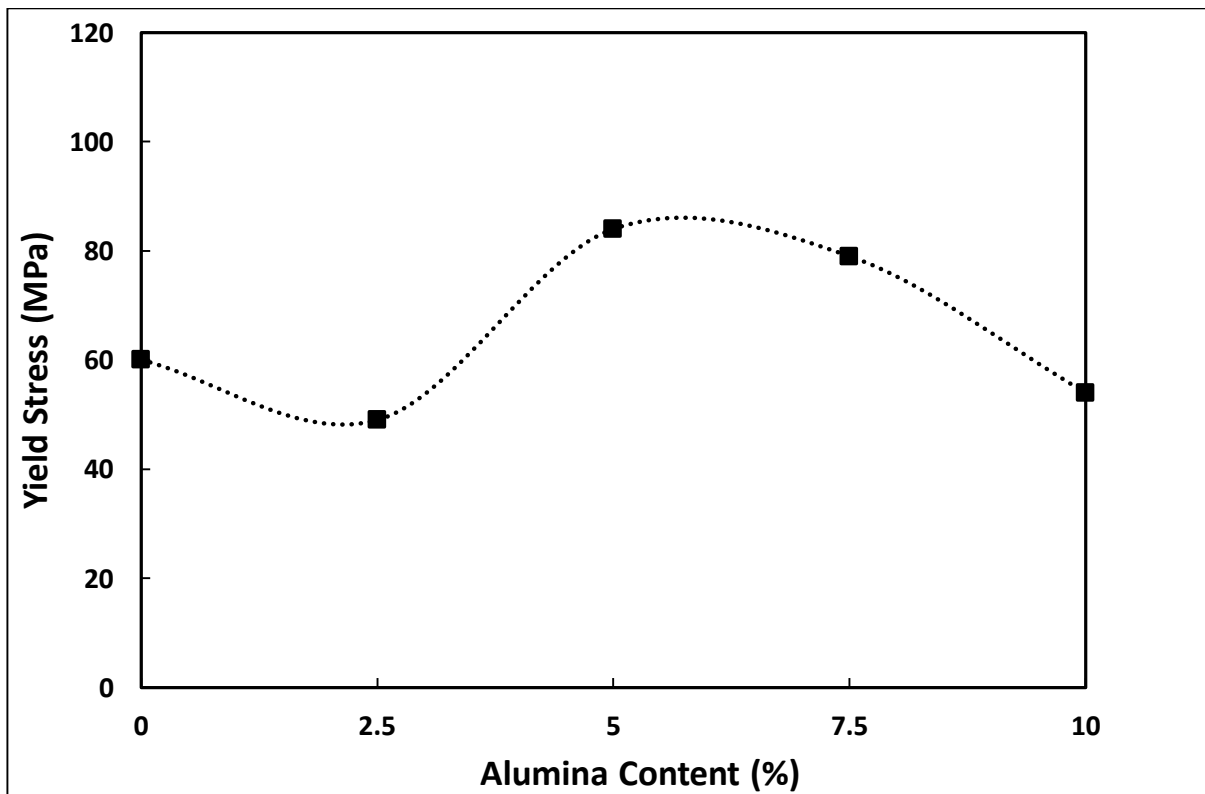


Fig. 9- Variation in the yield strength of the composites with different weight fractions of Al₂O₃ nanoparticles

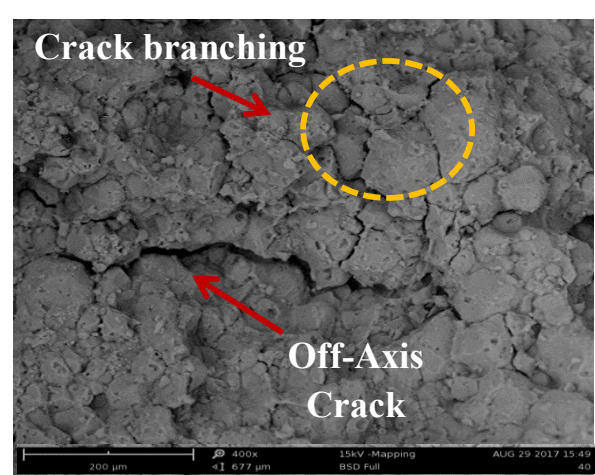
Fig. 10 shows the fracture surface of the compression test samples with and without added Al₂O₃ nanoparticles. Fig. 10 (a) shows the fracture surface of the pure aluminium sample without added nanoparticles. The surface showed a ductile failure with multiple narrow cracks moving along the grain boundaries due to the coalescence of micro-cavities. Fig. 10 (b) and (c) show the fracture surface of the samples with 2.5 and 5% weight fraction of added nanoparticles, respectively. The surfaces were found to have high density ductile cracking regions which were not found in the pure aluminium sample. The fracture surfaces of samples with 7.5 and 10% weight fraction of added nanoparticles showed several microcracks, crack branching, arrested cracks, and grains pull out, as shown in Fig. 10 (d) and (e). It can be said that the samples with a higher weight fraction of nanoparticles were brittle and showed multiple fracture regions. The high cohesive energy of agglomerates and clusters of the nanoparticles turned the samples brittleness and reduced their yield strength.



(a)



(b)



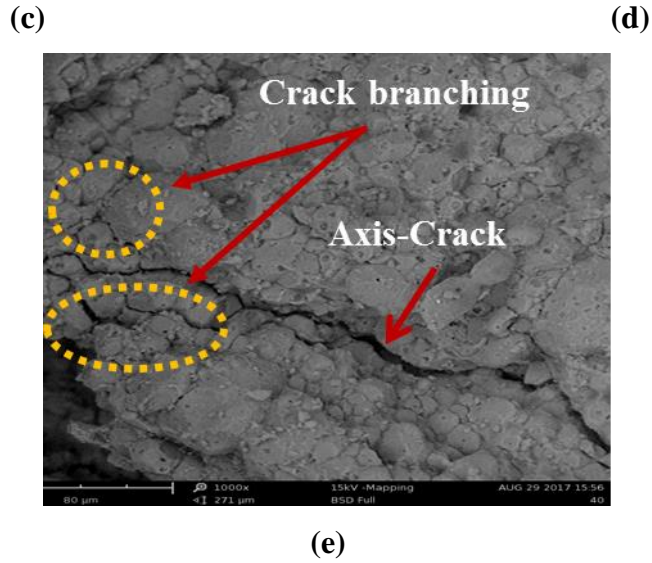


Fig. 10- SEM graphs of the fracture surface of specimens after quasi-static loading of aluminium matrix (a) without added Al₂O₃ (b) 2.5% Al₂O₃ (c) 5% Al₂O₃ (d) 7.5% Al₂O₃ and (e) 10% Al₂O₃

3.4. Dry sliding wear analysis

3.4.1. Effect of contact load on the coefficient of friction

The wear behaviour of the materials depends on their surface characteristics. The degradation and deformation of the surface of MMCs in contact loading vary with the weight fraction of Al₂O₃ nanoparticles in the matrix. The friction generates between the contact surface and pin, in the sliding test, controls the surface degradation of the material. Dry sliding wear tests were carried out on composite samples, with different weight fractions of Al₂O₃ nanoparticles, using 10, 15 and 20N contact load. The coefficient of friction between the material surface and the sliding pin was calculated as the ratio between lateral friction force and applied contact load given in eq. (1).

$$\mu = \frac{f}{L} = \frac{\text{lateral (friction) force}}{\text{normal (externally applied)load}} \quad (1)$$

Where μ is the coefficient of friction, f is the friction force and L is the applied contact load.

Fig. 11 shows the variation in the coefficient of friction between a composite sample with 5% weight fraction Al₂O₃ nanoparticles and a sliding pin for different contact loads. It was found that the coefficient of friction increased with the contact load. The higher penetration of the contact pin at a higher contact load offered more resistance to the sample in moving to lead to a higher coefficient of friction between the sample and pin. The coefficient of friction was

found to be 0.2 at 10N contact load which increased by 100% at 15N contact load and found to be 0.4. However, the coefficient of friction increased by only ~7% for a further 5N increase in the contact load from 15 to 20N. It can be said that initially, the coefficient of friction increased with a higher slope with an increase in the contact load. However, the coefficient of friction increased with a very moderate slope with a further increase in the contact loads. It can be said that variation in coefficient of friction was higher at lower contact loads than that at higher contact loads.

Fig. 12 shows the variation in the coefficient of friction between the material surface and sliding pin for different weight fractions of Al_2O_3 nanoparticles in the aluminium matrix. The coefficient of friction was higher in the samples without Al_2O_3 particles. The addition of Al_2O_3 nanoparticles in the material decreased the coefficient of friction between the sample surface and the pin. This trend was observed in samples up to 5% weight fraction of Al_2O_3 nanoparticles which showed the lowest coefficient of friction. It can be said that the addition of nanoparticles in the matrix forms thin films which act as the solid lubricant and reduce the coefficient of friction as mentioned in ⁴⁶. The coefficient of friction started to increase again with a further increase in the weight fraction of Al_2O_3 nanoparticles beyond 5% in the aluminium matrix. The increase in the coefficient of friction was proportionally higher as compared to samples with nanoparticles less than 5% weight fraction. For example, at 20N contact load, the decrease in coefficient of friction was ~10% with every 2.5% increase in the weight fraction of nanoparticles in the samples up to 5% weight fraction. However, the coefficient of friction increased by ~20% for every 2.5% further increase in the weight fraction of nanoparticles in the samples containing more than 5% weight fraction of nanoparticles.

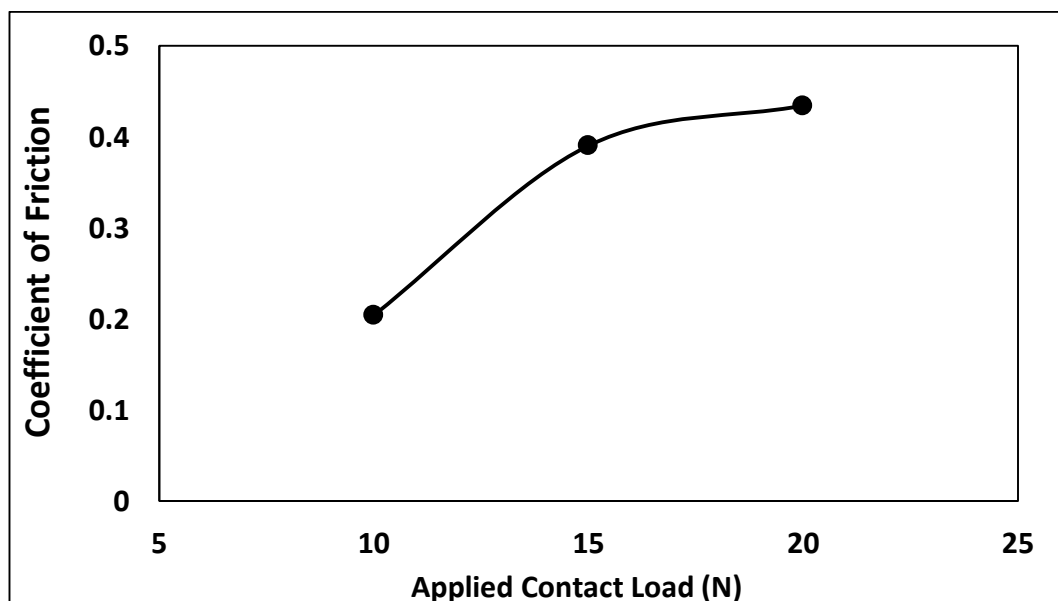


Fig. 11- Variation in the coefficient of friction for a sample with 5% Al₂O₃ with different contact loads

The increase in the weight fraction of nanoparticles increased the brittleness and agglomeration in the samples, decreasing the bonding between the aluminium and Al₂O₃ nanoparticles. The lower bond strength between the aluminium and Al₂O₃ nanoparticles resulted in grains pull out of nanoparticles from the aluminium matrix in the wear test and increased the coefficient of friction. It can be said that the samples with a higher weight fraction of nanoparticles offer more resistance to the pin in sliding and are more prone to scratch and fretting wear, loss of material, and interfacial bond breaking of nanoparticles with the matrix. The excessive percentage of hard nanoparticles in the aluminium matrix provided more resistance to the pin in sliding over the samples and produced a higher coefficient of friction. The sample surface found to have debris of removed particles from the matrix ⁴⁶.

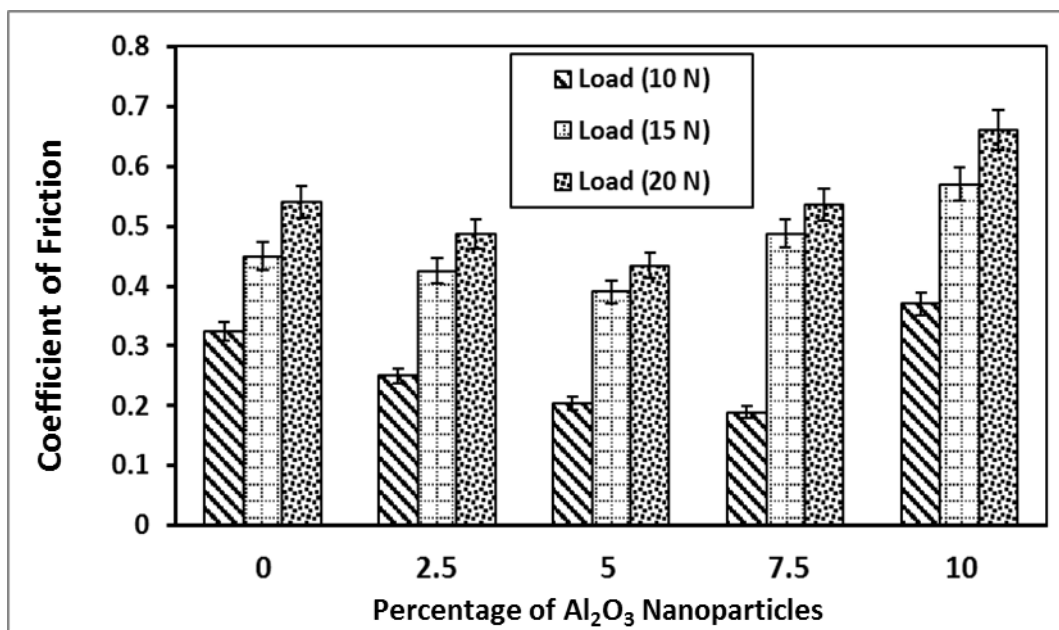


Fig. 12- Variation of the coefficient of friction in samples with different weight fractions of Al₂O₃ nanoparticles at different contact loads

3.5. Effect of load on wear loss of the samples

The wear loss of the material in the sliding wear test was calculated from the change in the weight of samples before and after the test. Fig. 12 shows the variation in the material loss in samples with different weight fractions of Al₂O₃ nanoparticles in the aluminium matrix at different applied contact loads. The material loss data is shown for sliding wear tests at 1.5 m/s speed for pin sliding distance 200 m. The sliding speed and distance were used to remain

consistent with previous studies on the material for validation of wear rate and deformation mechanism^{47, 48}. The material loss in the samples found to be higher in tests conducted at higher contact load. It can be said that a deeper penetration of the pin at higher contact loads produced a higher plastic deformation of the material in the scratching and sliding process resulting in more loss of material from the sample surface.

The material loss was found to be higher in the samples without Al₂O₃ nanoparticles and their addition in the matrix decreased the material loss in samples. The lowest material loss was found in the samples with 5% weight fraction of Al₂O₃ nanoparticles. It can be said that the addition of nanoparticles in the matrix caused a higher interfacial bonding between nanoparticles and the matrix. This led to a higher scratch resistance of the sample and lower material removal in the sliding wear test. The material loss in the samples started to increase again with a further increase of Al₂O₃ nanoparticles in the aluminium matrix beyond the 5% weight fraction. The increase in the material loss was significantly higher in samples with nanoparticles greater than 5% weight fraction. At 20N contact load, the decrease in material loss was ~10-15% with every 2.5% increase in the weight fraction of nanoparticles in the samples up to 5% weight fraction. However, the material loss increased by ~40-100% for a further every 2.5% increase in the weight fraction of nanoparticles in the samples beyond the optimum 5% weight fraction of nanoparticles.

The higher loss of material at higher contact loads showed that the scratch resistance of the composite material was significantly lower in samples with a higher weight fraction of Al₂O₃ nanoparticles than 5%. This was in agreement with previous studies which showed a higher wear rate of the MMCs at higher contact loads^{49, 50}. The significantly higher material loss of the samples with a higher weight fraction of Al₂O₃ nanoparticles than optimum level showed that the effects of excessive weight fraction of nanoparticles in the composite were more detrimental than having an insufficient weight fraction of nanoparticles in the composite. It can be said that agglomeration in samples with a higher weight fraction of nanoparticles than optimal weight fraction reduced the strength of samples. Furthermore, the weak bonding between nanoparticles and matrix in these samples increased the brittleness.

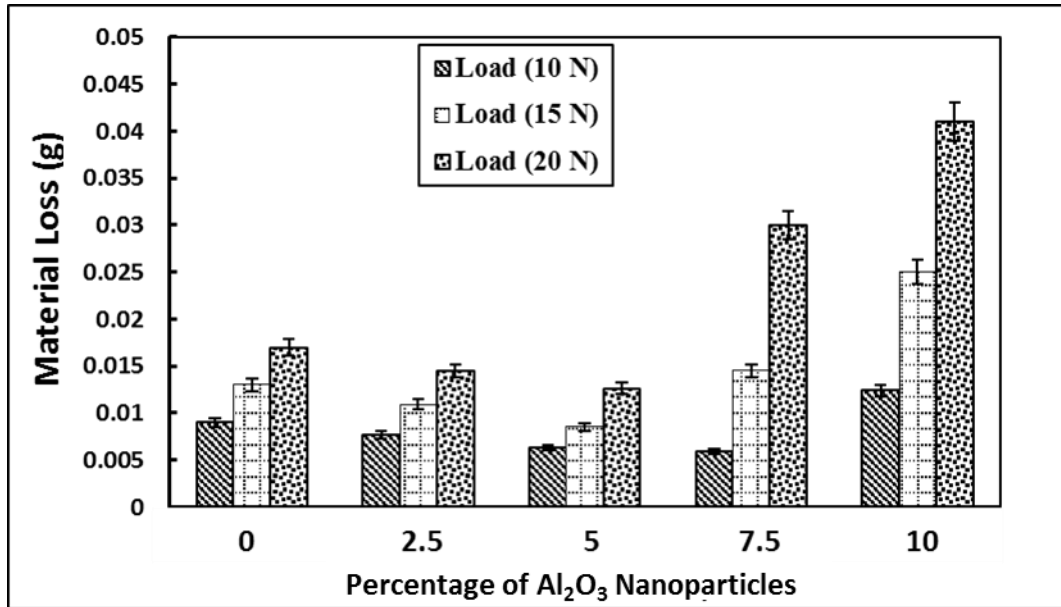
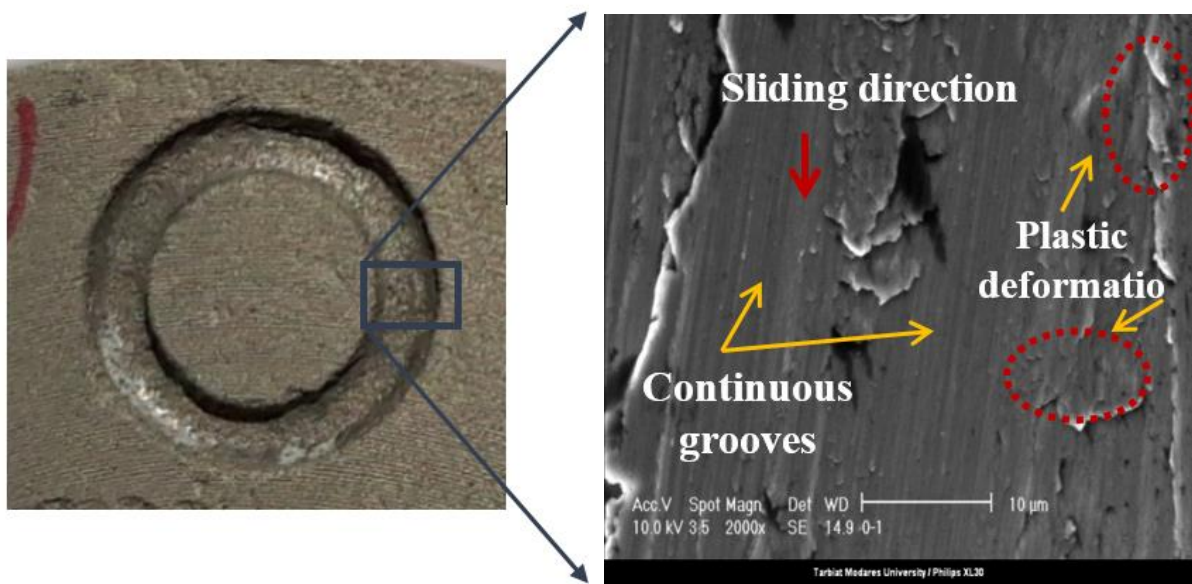


Fig. 13- Variation in the material loss in wear test with weight fraction of Al₂O₃ nanoparticles in the matrix

3.6. Worn surface analysis

The variation in the coefficient of friction and wear behaviour of the material with contact loads and weight fraction of nanoparticles was investigated by comparing the wear surface morphology in the samples. Fig. 13 (a) shows the wear trace on the samples in the sliding wear test at 15N contact load. The higher magnification images of surface morphology of material with different weight fraction of Al₂O₃ nanoparticles are shown in Fig. 13 (b) to (f). Fig. 13 (b) shows the wear surface of the sample without nanoparticles. The surface of the material was found to have small size grooves showing removal and abrasion of the aluminium. The material showed accumulated plastic shear flow on the surface of the sample. The addition of Al₂O₃ nanoparticles in the aluminium matrix affected the wear surface morphology. Fig. 13(c) and (d) show the wear surface of the samples with 2.5 and 5% weight fraction of nanoparticles, respectively. The worn surfaces in these samples were comparably smooth to those without nanoparticles. There were shallow grooves along the sliding direction on the surface of the samples. The lower density grooves on the surface of samples showed a higher scratch and wear resistance of the material which resisted against the plastic deformation and material flow. The shallow groove density was lower in the sample with 5% Al₂O₃ nanoparticles than in with 2.5% Al₂O₃ nanoparticles which showed a relatively higher wear resistance of the material.

Fig. 13 (e) and (f) show the worn surface of the sample with 7.5 and 10% weight fraction of nanoparticles, respectively. The plastic deformation of the surface showed evidence of ploughing of the material, cutting, and debris of material. The material removed in the sliding wear process was found to be ploughed around the sliding groove. The deeper sliding grooves in the samples showed their lower scratch and wear resistance which can be attributed to insufficient bonding, agglomeration of nanoparticles with matrix, and porosities in their microstructure. The nanoparticles squeezed out from the matrix in the scratching process and formed debris around the sliding track. The significantly higher material loss in these samples, as shown in Fig. 12, indicates that the weight fraction of Al_2O_3 nanoparticles in composite more than their optimum level is more detrimental than keeping an insufficient weight fraction of nanoparticles in the composite.



(a)

(b)

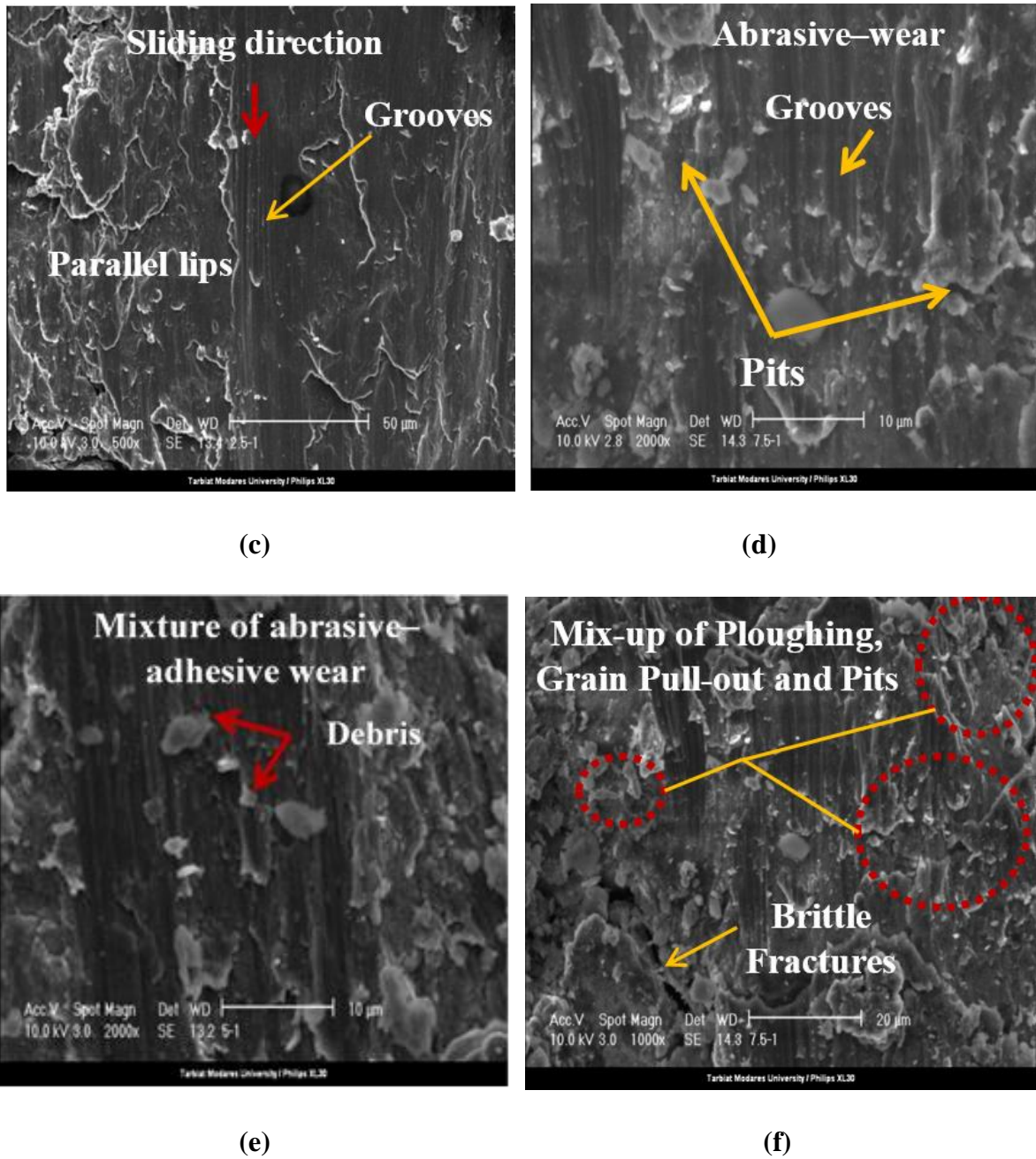


Fig. 14- SEM images of worn surface of the aluminium matrix and nanocomposites at 15 N sliding load (a) wear trace on the sample; part (b) to (f) shows surface of aluminium matrix samples with (b) no added Al_2O_3 (c) 2.5% Al_2O_3 (d) 5% Al_2O_3 (e) 7.5% Al_2O_3 and (f) 10% Al_2O_3

Fig. 15 (a) and (b) show the high magnification image of worn surface of samples with 5 and 10% weight fraction of nanoparticles, respectively, deformed at 20N contact load. It can be seen that in these samples the sliding mark, scratches, and grooves were deeper than those observed at 15N contact load as seen in ⁴⁹ the morphology of worn surfaces shows that ploughing and abrasion of the wear surface are considerably increased with increasing applied

load. The ploughing material was greater than that observed at the 15N contact load. The samples with a 10% weight fraction of nanoparticles showed a higher abrasive surface and brittleness. This showed that a higher weight fraction of nanoparticles in composite triggers brittleness in the material and show a severe loss in wear resistance of the material.

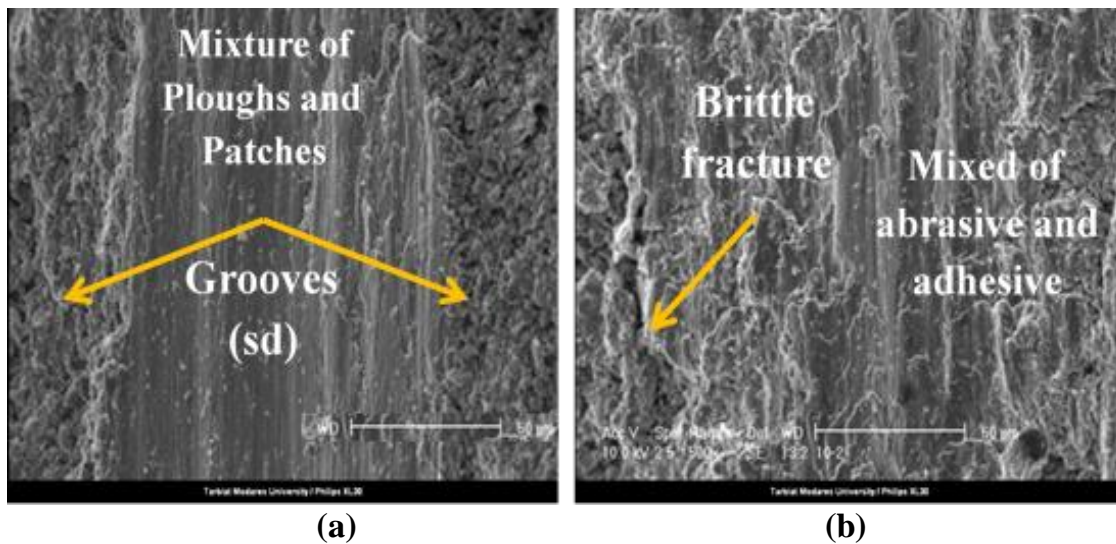


Fig. 15- Worn surfaces of composite samples at 20 N contact load for aluminium matrix with (a) 5%Al₂O₃(b) 10% Al₂O₃

It can be said that the wear resistance of the samples increases with the addition of nanoparticles in the matrix up to a limit. The maximum wear resistance was found in the material with a 5% weight fraction of nanoparticles. The addition of Al₂O₃ nanoparticles in the material beyond the 5% weight fraction decreases its wear resistance. This can be attributed to the limitation of the hard Al₂O₃ nanoparticles performance in the aluminium matrix. The plastic deformation of the material in the wear showed abrasion and adhesion of the surface. The aluminium matrix plastic deformation is ductile while Al₂O₃ nanoparticles on plastic deformation show brittle cracking. The insufficient bonding and agglomeration of nanoparticles with matrix in samples with a higher weight fraction of nanoparticles give rise to a lower scratch and wear resistance of the material. The excess nanoparticles in these samples squeeze out from the matrix in the scratching and sliding wear process.

Fig. 16 (a) and (b) show the variation in the debris of material formed in the sliding wear test of samples with and without nanoparticles, respectively. As shown in Fig. 16 (a), the aluminium samples without nanoparticles showed long chips and delamination scales on the surface. The material was found to have ductile damage with shallow grooves and debris particles. It can be said that the higher coefficient of friction between the aluminium sample

and pin produces high shear forces in the sliding wear process pulled out the debris of material and showed abrasive damage. A tape was used to collect the debris from the worn surface of the sample with a 5% weight fraction of Al_2O_3 nanoparticles. Fig. 16 (b) shows the SEM image of debris on that tape surface. The surface found to have uniformly distributed debris with lower abrasive damage. The lower abrasive wear damage observed in the sample can be attributed to the strong interfacial bonding of matrix and uniformly distributed nanoparticles.

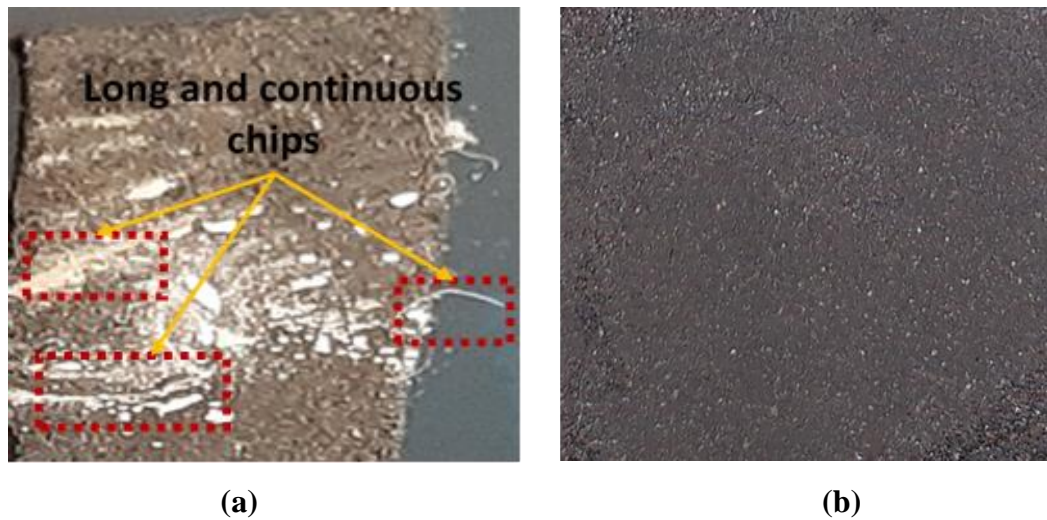


Fig. 16 Wear debris at 20N contact load in samples with (a) no Al_2O_3 (b) 5% Al_2O_3

3.7. Effect of sliding speed on material loss in wear

Fig. 17 shows the variation in loss of material with sliding speeds used in the wear test. It can be seen that material loss was higher at higher sliding speed and in those samples without added nanoparticles. The material loss decreased with the addition of nanoparticles in the samples to a 5% weight fraction. The addition of nanoparticles in the samples beyond the 5% weight fraction showed a higher material loss in the sliding wear test which was proportionally higher as compared to samples with nanoparticles less than 5% weight fraction. This showed that samples with a higher fraction of Al_2O_3 nanoparticles were prone to a higher material loss in high-speed fretting and sliding applications. The increase in the material loss was significantly higher in samples with nanoparticles greater than 5% weight fraction. Initially, the material loss decreased by ~15% with every 2.5% increase in the weight fraction of nanoparticles in the samples up to 5% weight fraction. However, the material loss increased by ~40-100% for every 2.5% further increase in the weight fraction of nanoparticles in the samples beyond the optimum 5% weight fraction of nanoparticles.

The higher weight fraction of nanoparticles in the material increases the hardness and brittleness of the materials which reduces the scratch and wear resistance of the material. The lower resistant brittle material deforms more at a higher sliding speed and showed a significant material loss. It can be said that a higher energy and contact temperature that develop at the higher sliding speed lead to the rapid oxidation of the matrix material and produce more material loss in the wear⁵¹⁻⁵³. It can be said that samples with a higher weight fraction of Al₂O₃ nanoparticles experience more material loss in composite and due to their higher brittleness and extremely poor wear resistance. The effects of a higher weight fraction of nanoparticles in the composite were more damaging than adding a lower weight fraction of nanoparticles in the matrix. The variation in sliding speed in the wear test showed that material loss from samples was higher for lower sliding speed tests^{29,52}. The wear at lower sliding speed results in abrasive wear of the surface resulting in deeper scratches on the worn surface. However, the higher sliding speed produces delamination and adhesion of the worn surface of the material.

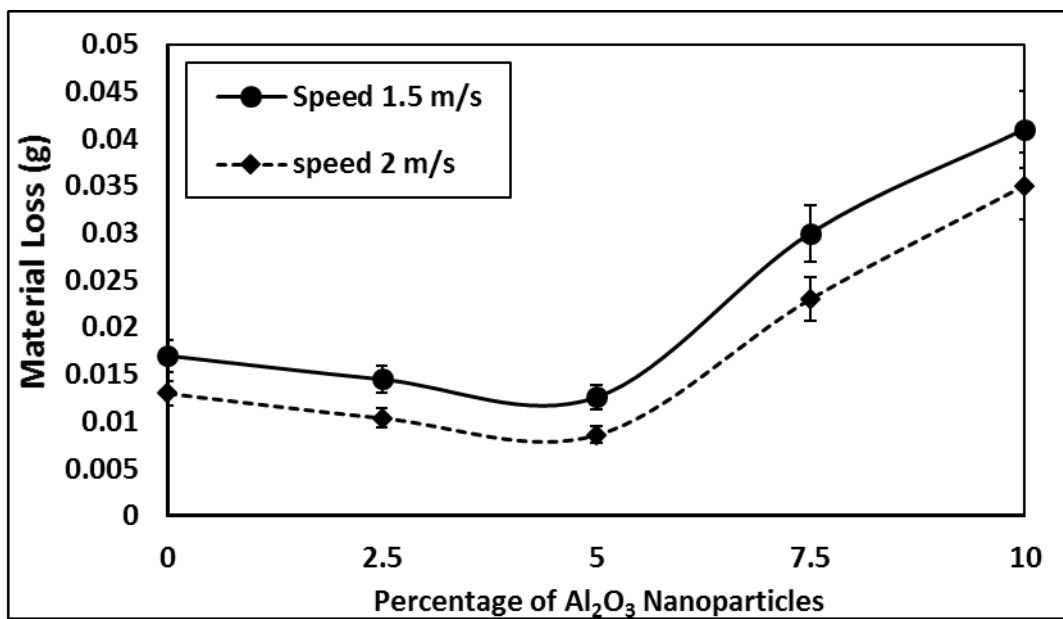


Fig. 17- Variation in the material loss of samples with weight fraction of Al₂O₃ nanoparticles at different sliding speeds

3.8. Micro-hardness of the composite

Fig. 18 shows the variation in the hardness of the material with the weight fraction of nanoparticles. It can be seen that the addition of nanoparticles linearly increased the hardness of the composite^{2,46}. The increase in hardness of the composite can be attributed to the addition of hard refined Al₂O₃ nanoparticles following the Hall-Petch theory^{37, 53}. The addition of nanoparticles in the matrix hinders the dislocation motion according to the Orowan mechanism

increasing the strength and hardness of the material ⁵¹. The higher weight fraction of Al₂O₃ nanoparticles in the composite increases the dislocation density of the matrix as observed in dislocation strengthening ².

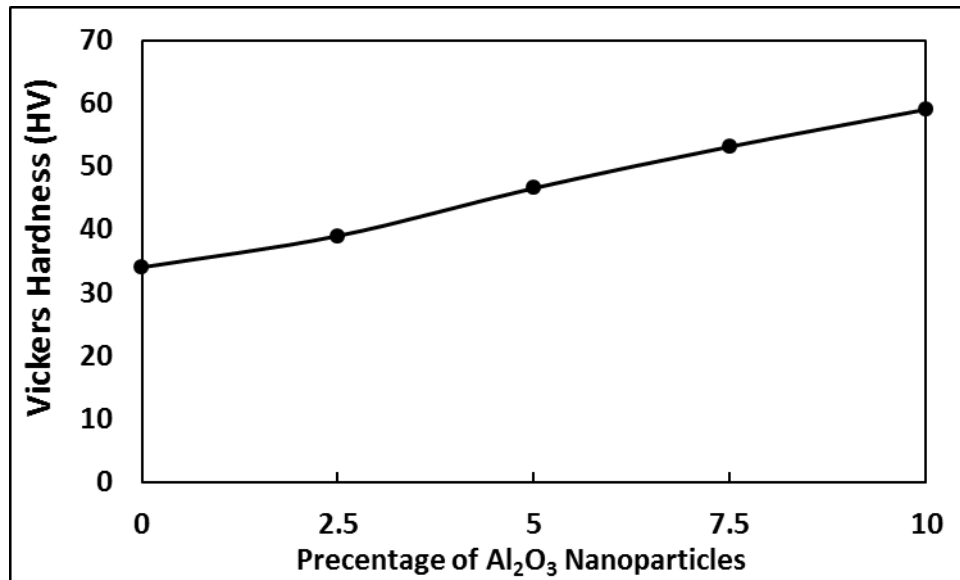


Fig. 18- Variation in the hardness of the composite with weight fraction of nanoparticles

The increase in hardness with the addition of nanoparticles in the composite reduced the material loss in the sliding wear test. However, the effect was observed only up to a 5% weight fraction of nanoparticles in the composite. The addition of nanoparticles in the samples beyond the 5% weight fraction increased the hardness of the composite however, an opposite effect was observed on the material loss of the composite. It can be said that the addition of nanoparticles up to a 5% weight fraction in the aluminium matrix increases the hardness of the composite which leads to a higher scratch and wear resistance of the composite. Further addition of Al₂O₃ nanoparticles increased the hardness but that increase changed the sliding wear mechanism of the composite and adversely affects the performance of the material. The higher brittleness of the material, due to the excessive addition of Al₂O₃ nanoparticles, produced a significantly higher material loss in the wear load. It can be said that only an increase in hardness can be misleading for the prediction of the performance of the MMCs in fretting and wear applications.

The addition of Al_2O_3 nanoparticles in the aluminium matrix yields two different wear mechanisms of the composite. The Al_2O_3 nanoparticles in the aluminium matrix in the optimum range help in developing a tribological layer that augments the sliding between the sample and scratching pin. However, excess addition of Al_2O_3 nanoparticles in the aluminium matrix form a brittle composite which becomes more prone to abrasive failure of the material surface. It can be said that an optimum weight fraction of the aluminium oxide nanoparticles in the composite result in higher static yield strength, hardness, scratch resistance and lower material loss in wear and improve the mechanical performance of the material in quasi-static and sliding wear loading. The addition of nanoparticles beyond optimal weight fraction adversely affects the performance of the material due to increased brittleness. The material properties of the composite were found to be more sensitive to the weight fraction of nanoparticles beyond the optimum level. The Al_2O_3 nanoparticles in the aluminium matrix beyond the optimum level show a severe loss in wear properties as compared to adding a lower weight fraction of nanoparticles which has marginal consequences. It can be concluded that careful investigation of the fracture and deformation behaviour of composite led weight fraction selection of nanoparticles in the matrix can produce the MMC of higher compressive strength, hardness, and wear resistance. The MMC developed can be used effectively in engineering applications where higher strength, friction, and scratch resistance of the material are required. The mechanistic understanding of the role of Al_2O_3 nanoparticles in the aluminium matrix in static and wear load will be used in the future for the development of a mathematical model for the prediction of the material properties of nanoparticles reinforced MMCs.

4. Conclusion

Powder metallurgy was used to produce composite specimens by adding different weight fractions of Al_2O_3 nanoparticles in the aluminium matrix. It was found that the addition of Al_2O_3 nanoparticles in the aluminium matrix produces composites with uniform distribution of reinforced particles in the matrix which helps in achieving the consistent mechanical properties of the material in static and wear load. The effects of variation in aluminium oxide nanoparticles in aluminium-based metal matrix composite on the compressive and sliding wear deformation showed that an optimum weight fraction of nanoparticles in composite increase the quasi-static and sliding wear performance of the material. The 5% weight fraction of Al_2O_3 nanoparticles was found to be the optimal weight fraction which showed significantly higher compressive yield strength, hardness, scratch resistance, and lower material loss in wear. The addition of nanoparticles beyond optimal weight fraction adversely affects the performance of

the composite and the effects were more detrimental than those with a lower weight fraction of nanoparticles. The material showed an increase in the coefficient of friction with an increase in the applied contact load. The wear rate of the material was found to be higher at higher contact loads. The increase in sliding speed showed a lower wear rate of the material.

Competing interest statement

The authors declare that they have no competing financial interests.

5. Reference

1. Tiku V, Navin K, Kurchania R. Study of Structural and Mechanical Properties of Al/Nano-Al₂O₃ Metal Matrix Nanocomposite Fabricated by Powder Metallurgy Method. *Transactions of the Indian Institute of Metals*. 2020; 1-7.
2. Kallip K, Babu NK, AlOgab KA, et al. Microstructure and mechanical properties of near net shaped aluminium/alumina nanocomposites fabricated by powder metallurgy. *Journal of Alloys and Compounds*. 2017; 714: 133-43.
3. Idrisi AH, Mourad A-HI. Wear Performance Analysis of Aluminum Matrix Composites and Optimization of Process Parameters Using Statistical Techniques. *Metallurgical and Materials Transactions A*. 2019; 50: 5395-409.
4. Meselhy AF, Reda MM. Investigation of mechanical properties of nanostructured Al-SiC composite manufactured by accumulative roll bonding. *Journal of Composite Materials*. 2019; 53: 3951-61.
5. Nalivaiko AY, Arnautov AN, Zmanovsky SV, Ozherelkov DY, Shurkin PK, Gromov AA. Al–Al₂O₃ powder composites obtained by hydrothermal oxidation method: Powders and sintered samples characterization. *Journal of Alloys and Compounds*. 2020; 825: 154024.
6. Gudlur P, Forness A, Lentz J, Radovic M, Muliana A. Thermal and mechanical properties of Al/Al₂O₃ composites at elevated temperatures. *Materials Science and Engineering: A*. 2012; 531: 18-27.
7. Singh J, Chauhan A. Overview of wear performance of aluminium matrix composites reinforced with ceramic materials under the influence of controllable variables. *Ceramics International*. 2016; 42: 56-81.
8. Dwivedi SP, Srivastava AK, Maurya NK, Sahu R, Tyagi A, Maurya R. Microstructure and mechanical behaviour of Al/SiC/Al₂O₃ hybrid metal matrix composite. *Materials Today: Proceedings*. 2020; 25: 789-92.
9. Madhu HC, Edachery V, Lijesh KP, Perugu CS, Kailas SV. Fabrication of Wear-Resistant Ti₃AlC₂/Al₃Ti Hybrid Aluminum Composites by Friction Stir Processing. *Metallurgical and Materials Transactions A*. 2020; 51: 4086-99.
10. Farshbaf Ahmadipour M, Movahedi M, Kokabi AH. Microstructural Evaluation and Mechanical Properties of Al₁₀Si_{0.5}/TiO₂-Graphite Hybrid Nanocomposite Produced Via Friction Stir Processing. *Metallurgical and Materials Transactions A*. 2019; 50: 2443-61.

11. Samal P, Vundavilli PR, Meher A, Mahapatra MM. Recent progress in aluminum metal matrix composites: A review on processing, mechanical and wear properties. *Journal of Manufacturing Processes*. 2020; 59: 131-52.
12. Sharma VK, Kumar V, Joshi RS. Effect of RE addition on wear behavior of an Al-6061 based hybrid composite. *Wear*. 2019; 426-427: 961-74.
13. Hsieh C-T, Ho Y-C, Wang H, Sugiyama S, Yanagimoto J. Mechanical and tribological characterization of nanostructured graphene sheets/A6061 composites fabricated by induction sintering and hot extrusion. *Materials Science and Engineering: A*. 2020; 786: 138998.
14. Liu X-l, Cai Z-b, xiao Q, Shen M-x, Yang W-b, Chen D-y. Fretting wear behavior of brass/copper-graphite composites as a contactor material under electrical contact. *International Journal of Mechanical Sciences*. 2020; 184: 105703.
15. Paidpilli M, Gupta GK, Upadhyaya A. Effect of matrix powder and reinforcement content on tribological behavior of particulate 6061Al-TiB₂ composites. *Journal of Composite Materials*. 2018; 53: 1181-95.
16. Lü L, Lai MO, Liang W. Magnesium nanocomposite via mechanochemical milling. *Composites Science and Technology*. 2004; 64: 2009-14.
17. Harichandran R, Selvakumar N. Microstructure and mechanical characterization of (B₄C+ h-BN)/Al hybrid nanocomposites processed by ultrasound assisted casting. *International Journal of Mechanical Sciences*. 2018; 144: 814-26.
18. Karpasand F, Ardestani M, Abbasi A. The effect of powder addition manner and volume fraction of reinforcement on tribological behavior of Al7075/B₄C surface composite produced by friction stir processing. *Journal of Composite Materials*. 2020; 54: 2873-86.
19. Zaiemyekheh Z, Liaghat G, Ahmadi H, Khan M, Razmkhah OJMS, A E. Effect of strain rate on deformation behavior of aluminum matrix composites with Al₂O₃ nanoparticles. 2019.
20. San Marchi C, Cao F, Kouzeli M, Mortensen A. Quasistatic and dynamic compression of aluminum-oxide particle reinforced pure aluminum. *Materials Science and Engineering: A*. 2002; 337: 202-11.
21. Xiao J, Shu DW, Wang XJ. Effect of strain rate and temperature on the mechanical behavior of magnesium nanocomposites. *International Journal of Mechanical Sciences*. 2014; 89: 381-90.
22. Kaybal HB, Ulus H, Demir O, Şahin ÖS, Avcı A. Effects of alumina nanoparticles on dynamic impact responses of carbon fiber reinforced epoxy matrix nanocomposites. *Engineering Science and Technology, an International Journal*. 2018; 21: 399-407.
23. Mohammed MMM, Elkady OA, Abdelhameed AW. Effect of Alumina Particles Addition on Physico-Mechanical Properties of AL-Matrix Composites %J Open Journal of Metal. 2013; Vol.03No.04: 8.
24. Rahimian M, Parvin N, Ehsani N. Investigation of particle size and amount of alumina on microstructure and mechanical properties of Al matrix composite made by powder metallurgy. *Materials Science and Engineering: A*. 2010; 527: 1031-8.
25. Eltaher MA, A.Wagih, Melaibari A, Fathy A, Lubineau G. Effect of Al₂O₃ particles on mechanical and tribological properties of Al-Mg dual-matrix nanocomposites. *Ceramics International*. 2020; 46: 5779-87.
26. Al-Jaafari MAA. Study the effects of different size of Al₂O₃ nanoparticles on 6066AA and 7005AA composites on mechanical properties. *Materials Today: Proceedings*. 2021; 42: 2909-13.
27. Aydin F. The investigation of the effect of particle size on wear performance of AA7075/Al₂O₃ composites using statistical analysis and different machine learning methods. *Advanced Powder Technology*. 2021; 32: 445-63.
28. Bharath V, Auradi V, Nagral M, Dayanand S, Boppana SB. Impact of Alumina Particulates Addition on Hardness and Wear Behaviour of 2014 Al Metal Matrix Composites by Vortex Method. *IOP Conference Series: Materials Science and Engineering*. 2021; 1013: 012018.
29. Al-Qutub AM, Allam IM, Abdul Samad MA. Wear and friction of Al-Al₂O₃ composites at various sliding speeds. *Journal of Materials Science*. 2008; 43: 5797-803.

30. Rahimian M, Parvin N, Ehsani N. The effect of production parameters on microstructure and wear resistance of powder metallurgy Al–Al₂O₃ composite. *Materials & Design*. 2011; 32: 1031-8.
31. Lakshmikanthan A, Bontha S, Krishna M, Koppad PG, Ramprabhu T. Microstructure, mechanical and wear properties of the A357 composites reinforced with dual sized SiC particles. *Journal of Alloys and Compounds*. 2019; 786: 570-80.
32. Yadav S, Chichili DR, Ramesh KT. The mechanical response of a 6061-T6 Al/Al₂O₃ metal matrix composite at high rates of deformation. *Acta Metallurgica et Materialia*. 1995; 43: 4453-64.
33. Chichili D, Ramesh KJ, Jos, structures. Dynamic failure mechanisms in a 6061-T6 Al/Al₂O₃ metal—matrix composite. 1995; 32: 2609-26.
34. Kurt H, Arik H, Bagci C. Abrasive Wear, Structure, and Mechanical Aspects of Al–Al₂O₃ Composites Fabricated Using Various Mixing Media During P/M Routes. *Powder Metallurgy and Metal Ceramics*. 2016; 55: 141-51.
35. Daha MA, Nassef BG, Nassef MGA. Mechanical and Tribological Characterization of a Novel Hybrid Aluminum/Al₂O₃/RGO Composite Synthesized Using Powder Metallurgy. *Journal of Materials Engineering and Performance*. 2021; 30: 2473-81.
36. Gudlur P, Muliana A, Radovic MJCPBE. Effective thermo-mechanical properties of aluminum–alumina composites using numerical approach. 2014; 58: 534-43.
37. Ezatpour HR, Torabi Parizi M, Sajjadi SA, Ebrahimi GR, Chaichi A. Microstructure, mechanical analysis and optimal selection of 7075 aluminum alloy based composite reinforced with alumina nanoparticles. *Materials Chemistry and Physics*. 2016; 178: 119-27.
38. Shaik MA, Golla BR. Two body abrasion wear behaviour of Cu–ZrB₂ composites against SiC emery paper. *Wear*. 2020; 450-451: 203260.
39. Ramesh B, Senthilvelan T. Formability characteristics of aluminium based composites-a review. *International Journal of Engineering and Technology*. 2010; 2: 1.
40. Rahmani K, Majzoobi GH. The effect of particle size on microstructure, relative density and indentation load of Mg–B₄C composites fabricated at different loading rates. *Journal of Composite Materials*. 2019; 54: 2297-311.
41. Rahimian M, Ehsani N, Parvin N, Baharvandi Hr. The effect of particle size, sintering temperature and sintering time on the properties of Al–Al₂O₃ composites, made by powder metallurgy. *Journal of Materials Processing Technology*. 2009; 209: 5387-93.
42. Hadian M, Shahrajabian H, Rafiei M. Mechanical properties and microstructure of Al/(TiC+TiB₂) composite fabricated by spark plasma sintering. *Ceramics International*. 2019; 45: 12088-92.
43. Gurson AL. Continuum Theory of Ductile Rupture by Void Nucleation and Growth: Part I—Yield Criteria and Flow Rules for Porous Ductile Media. *Journal of Engineering Materials and Technology*. 1977; 99: 2-15.
44. Ma S, Yuan H. Damage evolution and modeling of sintered metals under multi-axial loading conditions. *Computational Materials Science*. 2013; 80: 123-33.
45. Ibrahim A, Abdallah M, Mostafa SF, Hegazy AA. An experimental investigation on the W–Cu composites. *Materials & Design*. 2009; 30: 1398-403.
46. Misra D, Barange S, Joardar H, et al. Comparative study on the tribological properties of laser post-treated and untreated AISI304 stainless steel matrix composite reinforced with hard ceramic particles (TiB₂–TiN–SiC) and prepared by ex-situ P/M route. *Ceramics International*. 2019; 45: 18852-64.
47. Zhang J, Alpas AT. Wear regimes and transitions in Al₂O₃ particulate-reinforced aluminum alloys. *Materials Science and Engineering: A*. 1993; 161: 273-84.
48. Kök M, Özdin K. Wear resistance of aluminium alloy and its composites reinforced by Al₂O₃ particles. *Journal of Materials Processing Technology*. 2007; 183: 301-9.
49. Singh J, Chauhan A. Investigations on dry sliding frictional and wear characteristics of SiC and red mud reinforced Al2024 matrix hybrid composites using Taguchi's approach. *Proceedings of the*

Institution of Mechanical Engineers, Part L: Journal of Materials: Design and Applications. 2018; 233: 1923-38.

50. Girish G, Anandakrishnan V. A study on the microstructure, hardness, and tribological behavior of aluminum-based metal–matrix composite fabricated through recursive friction stir processing. *Proceedings of the Institution of Mechanical Engineers, Part L: Journal of Materials: Design and Applications*. 2020: 1464420720976686.

51. Xiao P, Gao Y, Xu F, et al. Tribological behavior of in-situ nanosized TiB₂ particles reinforced AZ91 matrix composite. *Tribology International*. 2018; 128: 130-9.

52. Ravindran P, Manisekar K, Rathika P, Narayanasamy P. Tribological properties of powder metallurgy – Processed aluminium self lubricating hybrid composites with SiC additions. *Materials & Design*. 2013; 45: 561-70.

53. Arab M, Marashi SPH. Graphene Nanoplatelet (GNP)-Incorporated AZ31 Magnesium Nanocomposite: Microstructural, Mechanical and Tribological Properties. *Tribology Letters*. 2018; 66: 156.